

Deep Reasoning with Multi-scale Context for Salient Object Detection

Zun Li¹, Congyan Lang¹, Yunpeng Chen², Jun Hao Liew², Jiashi Feng²

¹Beijing Jiaotong University, ²National University of Singapore

lznus2018@gmail.com, cylang@bjtu.edu.cn, chenyunpeng@u.nus.edu, liewjunhao@u.nus.edu, elefjia@nus.edu.sg

Abstract

To detect and segment salient objects accurately, existing methods are usually devoted to designing complex network architectures to fuse powerful features from the backbone networks. However, they put much less efforts on the saliency inference module and only use a few fully convolutional layers to perform saliency reasoning from the fused features. However, should feature fusion strategies receive much attention but saliency reasoning be ignored a lot? In this paper, we find that weakness of the saliency reasoning unit limits salient object detection performance, and claim that saliency reasoning after multi-scale convolutional features fusion is critical. To verify our findings, we first extract multi-scale features with a fully convolutional network, and then directly reason from these comprehensive features using a deep yet light-weighted network, modified from ShuffleNet [45], to fast and precisely predict salient objects. Such simple design is shown to be capable of reasoning from multi-scale saliency features as well as giving superior saliency detection performance with less computation cost. Experimental results show that our simple framework outperforms the best existing method with 2.3% and 3.6% promotion for F-measure scores, 2.8% reduction for MAE score on PASCAL-S, DUT-OMRON and SOD datasets respectively.

1. Introduction

Salient object detection, which aims to identify the most visually conspicuous objects in an image, serves as a pre-processing step for a variety of computer vision application, including image segmentation[36], video compression[7], photo synthesis[2], and visual tracking [9]. Although significant progress has been made with various valuable methods[21, 10, 22], it still requires more efforts to accurately detect salient objects in complex image scenarios.

Traditional salient object detection methods [40, 29, 4] generally utilize hand-crafted features and heuristic clues, which are hard to describe high-level semantic objects and scenes. Recently, convolutional neural networks especially

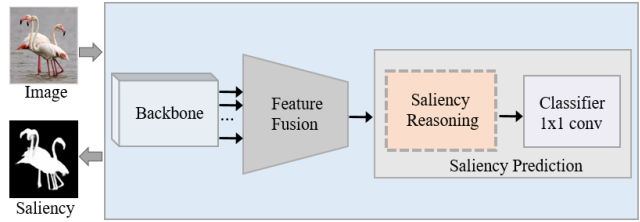


Figure 1: Illustration of existing FCN-based saliency detection framework. It usually includes three components: backbone network, feature fusion module and saliency prediction module. In this work, we focus on the *Saliency Reasoning* part which is the core of the saliency prediction module.

the fully convolutional networks (FCN) have been explored to overcome the drawbacks of the traditional saliency methods. The previous FCN-based saliency detectors typically consist of three components (i.e., backbone, feature fusion and saliency prediction), as shown in Figure 1. The backbone network usually produces a set of feature maps with decreasing spatial resolution. The feature fusion component aims to enhance these hierarchical features to better capture both distinctive objectness and local detailed information for detecting salient regions. After obtaining powerful multi-scale features, detectors predict saliency labels through two steps: one is saliency reasoning that is simply used for refining hierarchical features with a few fully convolutional layers; the other is a 1×1 convolution for differentiating saliency foreground and background parts. Among those components, the feature fusion gets a lot of attention for existing FCN-based saliency methods [34, 22, 42, 41, 33, 14, 23, 32]. To fuse more powerful features from each FCN layer, current detectors give great lengths to design complex network structures, and significant progress has been made with these methods. However, performance boost among those feature fusion-based saliency methods [22, 10, 33, 34, 1] tends to be saturated, leading to a bottleneck for designing accurate saliency detectors.

Several recent saliency methods [10, 6, 1] try to fuse multi-scale features via short connection and intermediate

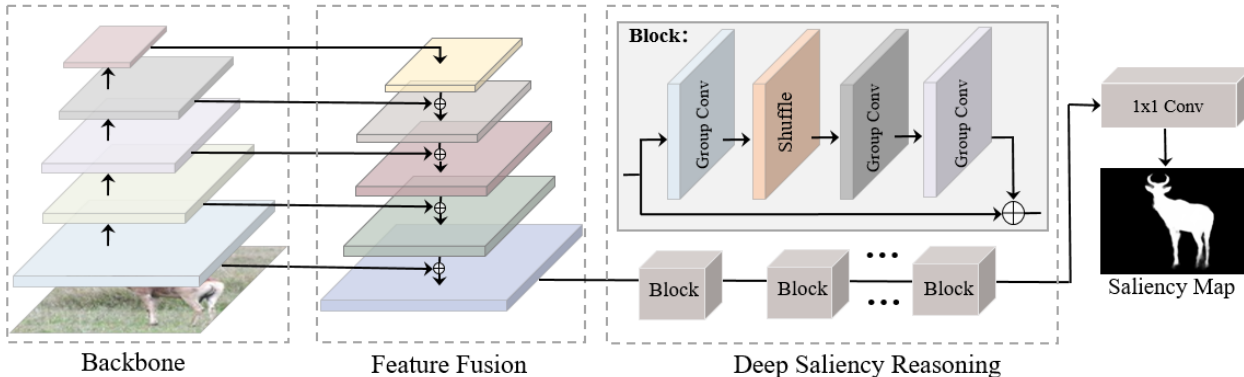


Figure 2: An instantiated framework for supporting our saliency reasoning in salient object detection. This architecture first fuses comprehensively saliency features of backbone feature extraction networks with upsampling and concatenate procedure, and then directly reason these features via designing a deep enough modified shuffleNet network.

supervision at each FCN layer. Only a few fully convolutional filters are adopted to reason combined features for saliency prediction. Despite impressive results from them, the improvements seemed to achieve saturation, because of the dependency of deep supervision as well as the weakness of saliency reasoning units. Thus, to obtain accurate saliency detection method, do we have to stick to these directions to increase complexity of fusion components?

In this work, we answer the above question and provide an alternative way to further boost saliency detection. We find that if the backbone network in Figure 1 is capable of extracting comprehensive multi-scale saliency clues, the most important issue becomes how to find a proper network architecture to maximally reason saliency information from these features. More recently, several methods are proposed to enhance the reasoning ability of a deep model. For example, [3][35] propose to use graph convolution to do the relation reasoning, while [20] propose to introduce second order terms to enhance the learning capacity of the network. Those methods are shown to be effective, yet complicated and may require some non-trivial modifications to be applicable to the saliency detection task.

In this work, we adopt a more straightforward solution by stacking convolution layers to build a deeper and larger saliency reasoning module. To reduce computation overhead from the deep reasoning modules and further accurately detect salient objects in complex image scenarios, we revisit some recently proposed light-weighted network (i.e., shufflenet [45] or mobileNet [27]), and propose a very simple but general network, as shown in Figure 2. More specifically, the designed reasoning module exploits some light-weighted point-wise group convolutions and depth-wise convolutions, which costs less flops while offering a superior saliency prediction accuracy. We first utilize any backbone network (e.g, ResNet [8], VGG [28]) to extract multi-scale saliency features, and then directly concatenate

these features using 1×1 convolutional filters and upsample operations following FPN network [19]. After feature fusion, we perform saliency reasoning by a deep yet light-weighted network, modified based on ShuffleNet [45] to fit those fusion saliency cues fast and accurately. The final saliency is predicted with a general 1×1 convolution. In short, the main contributions of this paper include:

- We show the importance of the “Saliency Reasoning” module for accurate salient object detection, which has been ignored for quite a long time by previous works. We believe this work paves a new direction to further saliency detection study.
- We propose a simple yet general and effective solution to implement saliency reasoning, which is capable of fitting multi-scale saliency features with less flops cost while having a superior saliency accuracy.
- We conduct comprehensive experiments to compare the network instantiated by our proposed reasoning module and recent state-of-the-art methods. Our simple network outperforms these competitors under various metrics significantly.

2. Methodology

We aim to enhance the ability of the “Saliency Reasoning” module for more accurate salient object detection. To achieve this, we first introduce some effective techniques that can be used for solving complex saliency reasoning tasks by simply increasing the network depth. Then we describe an instantiation framework to verify the importance of saliency reasoning in saliency detection.

2.1. Deep Saliency Reasoning

Existing deep-learning-based saliency detectors usually perform saliency reasoning via a few regular convolutional

layers. This shallow network is only effective for solving simple reasoning tasks, while not applicable to complex reasoning problem because of the insufficient representation ability. A straightforward way to realize complex reasoning is to increase the depth and build a deeper and wider ‘‘Saliency Reasoning’’ module. However, increasing the depth by simply stacking regular 3×3 or 1×1 convolution layers will lead to high computational cost and over-fitting problem.

Recently, pursuing the best accuracy in very limited computational budgets at tens or hundreds of MFLOPs, thus the light-weighted networks become more and more popular. Different from the regular convolutional neural networks, those deep light-weighted architectures are able to attain good performance with a smaller number of parameters, which is more suitable for complex reasoning. Among them, group convolution and depth-wise convolution are the widely used techniques since they can significantly reduce the computational cost while maintain high accuracy. In this work, we take the speed advantage of these special convolution layer to design our proposed saliency reasoning module for complex reasoning:

- (i) *Group Convolution*[13][12][37][45]: AlexNet is one of the first work that adopts the group convolution, where the input tensor and output tensor are equally sliced into chunks along the channel dimension resulting in a set of groups. The connections between different groups are removed compared with regular convolution layers and only the connections within the group are kept. This leads to a sparsely connected convolution layer, which helps reduce both the computational cost and the model size.
- (ii) *Depth-wise Convolution* [5] [11] [27][24]: The depth-wise convolution can be seen as a special case of group convolution, where the number of group equals to the number of channels. In other words, a spatial convolution performed independently over each channel of an input.

Given a convolution layer with input/out channel dimension of C , the regular convolution layer has a complexity of $O(C^2)$, the group convolution has a complexity of $O(C/num_group)$, while the depth-wise convolution has a complexity of $O(C)$. Thus, adopting these sparse convolutions (in-cooperate with activation function) can help increasing the reasoning ability of the network without introducing significant computational overhead.

Our experiments show that a very deep light-weighted network with group convolution and depth-wise Convolution can well process saliency reasoning.

2.2. Framework Instantiation

We enhance the saliency reasoning ability for detecting salient regions by adopting computational efficient depth-wise convolutional layers. Specifically, we instantiate a deep depth-wise convolution based saliency reasoning network, namely SRNet, for accurate saliency detection. The overall framework is shown in Figure 2. Concretely, we first extract multi-scale saliency features with backbone network, such as the well-known ResNet [8], VGG [28] with the last classification layer removed. Then these low-resolution features with rich semantics are fused with high-resolution but semantically weak features via a top-down pathway and lateral connections. Within the fusion of each adjacent layers, each path is convolved with 1×1 convolution kernels and upsampled to the highest resolution among the paths. After feature fusion, SRNet employs a strong saliency reasoning component. A deep light-weighted network is designed inspired by the depth-wise convolution network: ShuffleNet [45]. In this network, we do some modifications of ShuffleNet to better design saliency reasoning module for saliency detection. Finally, a 1×1 convolution is used for the reasoning features to predict saliency values for each pixel.

3. Experiment

3.1. Setup

Datasets. To evaluate the effectiveness of the instantiation model, we conduct comprehensive experiments on six widely used saliency detection benchmark datasets, including ECSSD [38], PASCAL-S [18], DUTOMRON [39], HKU-IS [15], SOD [26] and DUTS-test [31]. These datasets consist of 1000, 850, 5168, 4447, 300 and 5019 natural complex images with manually labeled pixel-wise ground-truth.

Evaluation Metrics. We adopt the widely used precision-recall (PR) curves, max F-measure (F_β -max), and mean absolute error (MAE) as our evaluation metrics. Given a predicted saliency map with continuous probability values, we convert it into binary maps with arbitrary thresholds first, and then computing corresponding precision/recall values. The mean precision/recall pairs can be calculated by averaging precision/recall values over all images in a dataset. Following those precision/recall values, F-measure is an overall performance measurement, which is calculated as:

$$F_\beta = \frac{(1 + \beta^2) \times Precision \times Recall}{\beta^2 \times Precision + Recall}, \quad (1)$$

here, we set β^2 to 0.3 to emphasize more on precision. Besides, we follow recent studies [42, 44, 10, 21, 34, 43, 23, 1, 6] to report max F_β (F_β -max) across different thresholds for

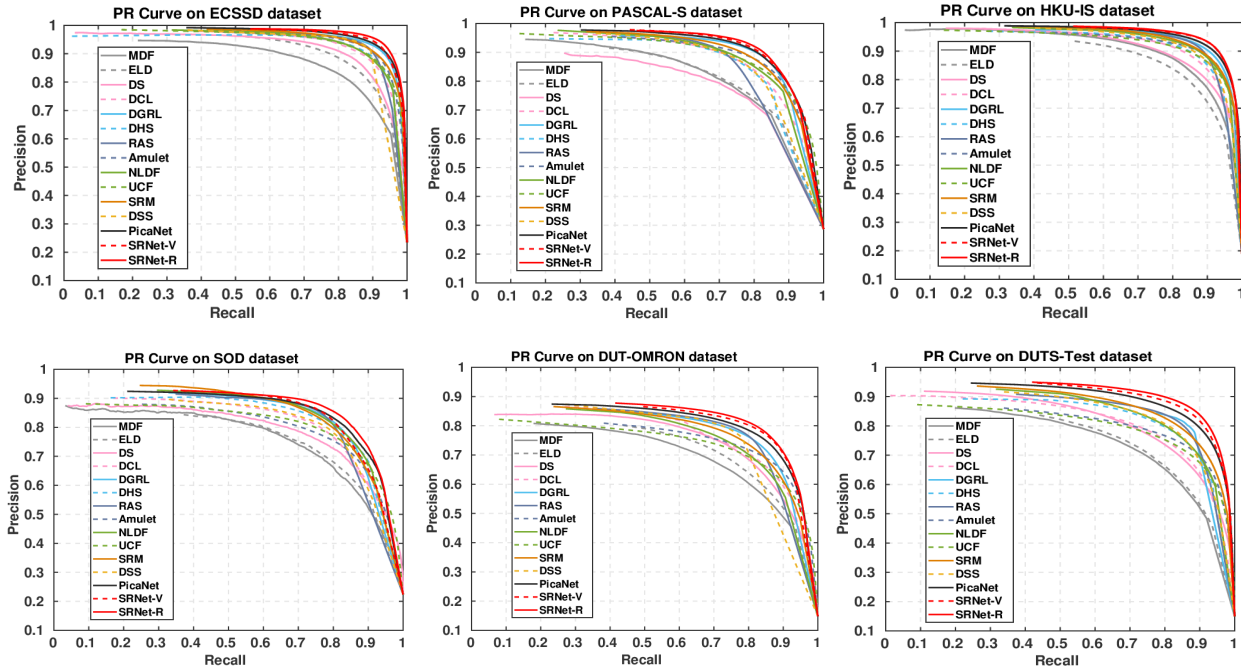


Figure 3: Quantitative results of PR curves for the instantiated model and other state-of-the-art models. The designed models of SRNet-V and SRNet-R that take VGG16 [28] and ResNet [8] as backbone respectively, they consistently outperform other models across most of the testing datasets.

evaluating our instantiation model and state-of-the-art models. The MAE is defined as the average pixelwise absolute difference between the saliency map S and its corresponding ground-truth G :

$$MAE = \frac{1}{W \times H} \sum_{x=1}^W \sum_{y=1}^H |S(x, y) - G(x, y)|, \quad (2)$$

where W and H represent the width and height of saliency map S respectively. $S(x, y)$ refers the saliency score at location (x, y) , and $G(x, y)$ is similar to $S(x, y)$.

3.2. Performance Comparison

In this manuscript, we simple compare an instantiation saliency detection model in Figure 2 with recent proposed 15 baseline methods, including MDF [16], LEGS [30], DCL [17], RFCN [32], DHS [21], DSS [10], NLDF [23], Amulet [42], SRM [33], RAS [1], DGRL [34], R3Net [6], BPPM [41], PAGR [44] and PicaNet [22]. For a fair comparison, we adopt the comparison results provided by [25] for all the competitors. The DHS [16] results on the DUT-OMRON [39] dataset are not reported because DHS uses a part of DUT-OMRON for training. Same reason is applied for the PAGR [44] results on the SOD [26] dataset. In this manuscript, we report the results by taking the ResNet-101 [8] (i.e., SRNet-R) and VGG-16 [28] (i.e., SRNet-V) as backbone respectively. Figure 3 illustrates the PR curves,

while Table 1 reports the max F-measure and MAE scores. To be mentioned that, more detailed experiment results will be reported in our update manuscript.

As shown in Figure 3, the instantiation model achieves a better PR curve than all the other methods across all the datasets, demonstrating the superior performance of our instantiation model for saliency detection. From Table 1, we can clearly see that the instantiation model can significantly outperform other competitors in terms of F_β -max and MAE scores, which demonstrates the effectiveness of saliency reasoning implementation for saliency detection. Specifically, comparing the F_β -max scores with ResNet [8] backbone, the instantiation model are 0.9%, 1.8%, 1.1%, and 2.7% higher than the existing best method on the ECSSD, DUT-test, HKU-IS, DUT-OMRON datasets, respectively. As for the MAE metric, the instantiation model (SRNet-V and SRNet-R) still ranks first on almost all datasets. Especially, comparing to the existing overall best performance PicaNet [22], the MAE score decreases from 0.104 to 0.076 on the SOD dataset, and from 0.087 to 0.075 on the PASCAL-S dataset. These results further indicate the effectiveness of the instantiation model for saliency detection. On the other hand, the performance boost between different backbones, i.e., SRNet-R and SRNet-V, is much significant than PicaNet [22] with these two backbones, illustrating the robustness of the saliency reasoning for the

Methods	ECSSD [38]		PASCAL-S [18]		DUTS-test [31]		HKU-IS [15]		SOD [26]		DUT-OMRON [39]	
	F_{β} -max	MAE	F_{β} -max	MAE	F_{β} -max	MAE	F_{β} -max	MAE	F_{β} -max	MAE	F_{β} -max	MAE
VGG [28] backbone												
MDF [16]	0.832	0.105	0.768	0.146	0.730	0.094	0.861	0.129	0.787	0.159	0.694	0.092
LEGS [30]	0.827	0.118	0.762	0.155	0.655	0.138	0.766	0.119	0.734	0.196	0.669	0.133
DCL [17]	0.890	0.088	0.805	0.125	0.782	0.088	0.885	0.072	0.823	0.141	0.739	0.097
RFCN [32]	0.890	0.107	0.837	0.118	0.784	0.091	0.892	0.079	0.799	0.170	0.742	0.111
DHS [21]	0.907	0.059	0.829	0.094	0.807	0.067	0.890	0.053	0.827	0.128	-	-
DSS [10]	0.916	0.053	0.836	0.096	0.825	0.057	0.911	0.041	0.844	0.121	0.771	0.066
NLDF [23]	0.905	0.063	0.831	0.099	0.812	0.066	0.902	0.048	0.841	0.124	0.753	0.080
Amulet [42]	0.915	0.059	0.837	0.098	0.778	0.085	0.895	0.052	0.806	0.141	0.742	0.098
RAS [1]	0.921	0.056	0.837	0.104	0.831	0.060	0.913	0.045	0.850	0.124	0.786	0.062
BMPM [41]	0.929	0.045	0.862	0.074	0.851	0.049	0.921	0.039	0.855	0.107	0.774	0.064
PAGR [44]	0.927	0.061	0.856	0.093	0.855	0.056	0.918	0.048	-	-	0.771	0.071
PicaNet [22]	0.931	0.047	0.868	0.077	0.851	0.054	0.921	0.042	0.853	0.102	0.794	0.068
SRNet-V	0.938	0.045	0.868	0.078	0.869	0.047	0.929	0.038	0.851	0.084	0.802	0.067
ResNet [8] backbone												
SRM [33]	0.917	0.054	0.847	0.085	0.827	0.059	0.906	0.046	0.843	0.127	0.769	0.069
DGRL [34]	0.922	0.041	0.854	0.078	0.829	0.056	0.910	0.036	0.845	0.104	0.774	0.062
R3Net [34]	0.931	0.046	0.845	0.097	0.828	0.059	0.917	0.038	0.836	0.136	0.792	0.061
PicaNet-R [22]	0.935	0.047	0.881	0.087	0.860	0.051	0.919	0.043	0.858	0.109	0.803	0.065
SRNet-R	0.944	0.040	0.883	0.075	0.878	0.045	0.930	0.036	0.859	0.076	0.830	0.060

Table 1: Comparisons of max F-measure (F_{β} -max) and MAE values with 15 methods on 6 benchmark datasets. The top three results are highlighted in **red**, **green**, and **blue**, respectively.

designed instantiation model.

4. Conclusion

In this paper, we show that saliency reasoning after multi-scale convolutional features fusion is critical for accurate salient object detection. To verify our findings, we propose a simple yet general and effective solution to implement more powerful saliency reasoning using a deep yet light-weighted network, modified from ShuffleNet. This instantiated model is capable of fitting multi-scale saliency context with less flops cost while offering a superior saliency accuracy. Comprehensive experiments demonstrate that the simple instantiated model outperforms state-of-the-art approaches across various evaluation metrics.

References

- [1] S. Chen, X. Tan, B. Wang, and X. Hu. Reverse attention for salient object detection. In *ECCV*, pages 236–252, 2018.
- [2] T. Chen, M. M. Cheng, A. Shamir, A. Shamir, and S. M. Hu. Sketch2photo: internet image montage. In *ACM SIGGRAPH Asia*, 2009.
- [3] Y. Chen, M. Rohrbach, Z. Yan, S. Yan, J. Feng, and Y. Kalantidis. Graph-based global reasoning networks. *arXiv preprint arXiv:1811.12814*, 2018.
- [4] M.-M. Cheng, N. J. Mitra, X. Huang, P. H. S. Torr, and S.-M. Hu. Global contrast based salient region detection. *TPAMI*, 37(3):569–582, 2015.
- [5] F. Chollet. Xception: Deep learning with depthwise separable convolutions. 2016.
- [6] Z. Deng, X. Hu, L. Zhu, X. Xu, J. Qin, G. Han, and P.-A. Heng. R³Net: Recurrent residual refinement network for saliency detection. In *IJCAI*, pages 684–690, 2018.
- [7] C. Guo and L. Zhang. A novel multiresolution spatiotemporal saliency detection model and its applications in image and video compression. *Oncogene*, 3(5):523–9, 1988.
- [8] K. He, X. Zhang, S. Ren, and J. Sun. Deep residual learning for image recognition. In *CVPR*, pages 770–778, 2015.
- [9] S. Hong, T. You, S. Kwak, and B. Han. Online tracking by learning discriminative saliency map with convolutional neural network. In *International Conference on Machine Learning*, 2015.
- [10] Q. Hou, M.-M. Cheng, X. Hu, A. Borji, Z. Tu, and P. Torr. Deeply supervised salient object detection with short connections. In *CVPR*, pages 5300–5309, 2017.
- [11] A. G. Howard, M. Zhu, C. Bo, D. Kalenichenko, W. Wang, T. Weyand, M. Andreetto, and H. Adam. Mobilenets: Efficient convolutional neural networks for mobile vision applications. 2017.
- [12] F. N. Iandola, S. Han, M. W. Moskewicz, K. Ashraf, W. J. Dally, and K. Keutzer. Squeezenet: Alexnet-level accuracy with 50x fewer parameters and 0.5mb model size. 2016.
- [13] A. Krizhevsky, I. Sutskever, and G. E. Hinton. Imagenet classification with deep convolutional neural networks. In *Advances in neural information processing systems*, pages 1097–1105, 2012.
- [14] G. Lee, Y.-W. Tai, and J. Kim. Deep saliency with encoded low level distance map and high level features. In *CVPR*, pages 660–668, 2016.
- [15] G. Li and Y. Yu. Visual saliency based on multiscale deep features. In *CVPR*, pages 5455–5463, 2015.

- [16] G. Li and Y. Yu. Visual saliency based on multiscale deep features. In *CVPR*, pages 5455–5463, 2015.
- [17] G. Li and Y. Yu. Deep contrast learning for salient object detection. In *CVPR*, pages 478–487, 2016.
- [18] Y. Li, X. Hou, C. Koch, J. M. Rehg, and A. L. Yuille. The secrets of salient object segmentation. In *CVPR*, pages 280–287, 2014.
- [19] T. Y. Lin, P. Dollr, R. Girshick, K. He, B. Hariharan, and S. Belongie. Feature pyramid networks for object detection. *CoRR*, abs/1612.03144, 2016.
- [20] T.-Y. Lin, A. RoyChowdhury, and S. Maji. Bilinear cnn models for fine-grained visual recognition. In *Proceedings of the IEEE International Conference on Computer Vision*, pages 1449–1457, 2015.
- [21] N. Liu and J. Han. Dhsnet: Deep hierarchical saliency network for salient object detection. In *CVPR*, pages 678–686, 2016.
- [22] N. Liu, J. Han, and M.-H. Yang. Picanet: Learning pixel-wise contextual attention for saliency detection. In *CVPR*, pages 3089–3098, 2018.
- [23] Z. Luo, A. K. Mishra, A. Achkar, J. A. Eichel, S. Li, and P.-M. Jodoin. Non-local deep features for salient object detection. In *CVPR*, pages 6593–6601, 2017.
- [24] N. Ma, X. Zhang, H. T. Zheng, and J. Sun. Shufflenet v2: Practical guidelines for efficient cnn architecture design. 2018.
- [25] Mengyang Feng. Evaluation toolbox for salient object detection. https://github.com/ArcherFMY/sal_eval_toolbox, 2018.
- [26] V. Movahedi and J. H. Elder. Design and perceptual validation of performance measures for salient object segmentation. In *CVPRW*, pages 49–56, 2010.
- [27] M. Sandler, A. Howard, M. Zhu, A. Zhmoginov, and L. C. Chen. Mobilenetv2: Inverted residuals and linear bottlenecks. 2018.
- [28] K. Simonyan and A. Zisserman. Very deep convolutional networks for large-scale image recognition. *CoRR*, abs/1409.1556, 2018.
- [29] J. Wang, H. Jiang, Z. Yuan, M. M. Cheng, X. Hu, and N. Zheng. Salient object detection: A discriminative regional feature integration approach. *International Journal of Computer Vision*, 123(2):1–18, 2017.
- [30] L. Wang, H. Lu, X. Ruan, and M.-H. Yang. Deep networks for saliency detection via local estimation and global search. In *CVPR*, pages 3183–3192, 2015.
- [31] L. Wang, H. Lu, Y. Wang, M. Feng, D. Wang, B. Yin, and X. Ruan. Learning to detect salient objects with image-level supervision. In *CVPR*, 2017.
- [32] L. Wang, L. Wang, H. Lu, P. Zhang, and X. Ruan. Saliency detection with recurrent fully convolutional networks. In *ECCV*, pages 825–841, 2016.
- [33] T. Wang, A. Borji, L. Zhang, P. Zhang, and H. Lu. A stage-wise refinement model for detecting salient objects in images. In *ICCV*, pages 4019–4028, 2017.
- [34] T. Wang, L. Zhang, S. Wang, H. Lu, G. Yang, X. Ruan, and A. Borji. Detect globally, refine locally: A novel approach to saliency detection. In *CVPR*, pages 3127–3135, 2018.
- [35] X. Wang and A. Gupta. Videos as space-time region graphs. *arXiv preprint arXiv:1806.01810*, 2018.
- [36] Y. Wei, X. Liang, Y. Chen, X. Shen, M. M. Cheng, J. Feng, Y. Zhao, and S. Yan. Stc: A simple to complex framework for weakly-supervised semantic segmentation. *TPAMI*, 39(11):2314–2320, 2015.
- [37] S. Xie, R. Girshick, P. Dollr, Z. Tu, and K. He. Aggregated residual transformations for deep neural networks. *arXiv preprint arXiv:1611.05431*, 2016.
- [38] Q. Yan, L. Xu, J. Shi, and J. Jia. Hierarchical saliency detection. In *CVPR*, pages 1155–1162, 2013.
- [39] C. Yang, L. Zhang, H. Lu, X. Ruan, and M.-H. Yang. Saliency detection via graph-based manifold ranking. In *CVPR*, pages 3166–3173, 2013.
- [40] C. Yang, L. Zhang, H. Lu, R. Xiang, and M. H. Yang. Saliency detection via graph-based manifold ranking. In *CVPR*, pages 3166–3173, 2013.
- [41] L. Zhang, J. Dai, H. Lu, Y. He, and G. Wang. A bi-directional message passing model for salient object detection. In *CVPR*, pages 1741–1750, 2018.
- [42] P. Zhang, D. Wang, H. Lu, H. Wang, and X. Ruan. Amulet: Aggregating multi-level convolutional features for salient object detection. In *ICCV*, pages 202–211, 2017.
- [43] P. Zhang, D. Wang, H. Lu, H. Wang, and B. Yin. Learning uncertain convolutional features for accurate saliency detection. In *ICCV*, pages 212–221, 2017.
- [44] X. Zhang, T. Wang, J. Qi, H. Lu, and G. Wang. Progressive attention guided recurrent network for salient object detection. In *CVPR*, pages 714–722, 2018.
- [45] X. Zhang, X. Zhou, M. Lin, and S. Jian. Shufflenet: An extremely efficient convolutional neural network for mobile devices. 2017.